Available online at www.sciencedirect.com
SCIENCE DIRECT®
Journal of Photochemistry and Photobiology A: Chemistry 161 (2003) 35–42
Journal of Photochemistry and Photobiology A:Chemistry
www.elsevier.com/locate/jphotochem

Picosecond electron transfer dynamics in polymer systems in solutions: cellulose tris(9-ethylcarbazolyl-3-carbamate) and amylose tris(9-ethylcarbazolyl-3-carbamate)

Sazzadur R. Khan [a,b], Akira Itaya [a], Hiroshi Miyasaka [b,*], Tadashi Okada [b], Chiyo Yamamoto [c], Yoshio Okamoto [c]

[a] *Department of Polymer Science and Engineering, Kyoto Institute of Technology, Matsugasaki, Sakyo, Kyoto 606-8585, Japan*
[b] *Department of Chemistry, Graduate School of Engineering Science, Osaka University, Toyonaka, Osaka 560-8531, Japan*
[c] *Division of Chemistry, Graduate School of Engineering, Nagoya University, Chikusa, Nagoya 464-8603, Japan*

Received 10 January 2003; received in revised form 27 March 2003; accepted 12 May 2003

Abstract

Photoinduced electron transfer (ET) dynamics, such as charge separation (CS), charge recombination (CR), and hole transfer (HT) processes in cellulose tris(9-ethylcarbazolyl-3-carbamate) (CTCz) and amylose tris(9-ethylcarbazolyl-3-carbamate) (ATCz) with a guest electron acceptor in solutions were investigated by means of picosecond transient absorption spectroscopy. Each glucoside unit of these polymer chains has three carbazolyl (Cz) units in such a configuration that two of them are in a close proximity and the other stays apart. Hole transfer dynamics in these systems in the early stage following the excitation were analyzed on the basis of one-dimensional random walk model where cationic state migrates along the polymer chain. On the other hand, the deviation of the experimental results from the calculated curve based on the above model was observed in nanosecond time region. By integrating the kinetic profiles with the temporal evolution of the absorption spectra of the charge-separated state, the trapping process of the cation at the dimer site was found to be responsible for this deviation. By comparing the present results with those in the monomer and dimer model systems as well as in other Cz containing polymer systems, the role of dimer cation in the HT process was discussed.

Keywords: Photoinduced electron transfer; Hole transfer; Picosecond laser photolysis; Transient absorption; Hole trapping

1. Introduction

Photoinduced electron transfer (ET) and its subsequent processes play fundamental and important roles in a number of photochemical reactions in the condensed phase [1–6]. Transport of electrons initiated by photoexcitation is one of the phenomena closely related to the photoinduced ET and is ubiquitous in nature as well as in artificial systems. In the natural system, the photosynthetic reaction center in plants is a most representative system where the electron transport takes place efficiently in three-dimensional arrangements [5]. In the artificial system, a great deal of efforts has been devoted to the construction of organic photoconductive molecular systems [7,8]. Among these artificial systems, the vinyl polymer with large pendant aromatic groups is one of the most well-known materials and has been attracting much attention from various viewpoints [9–17].

Recently, we investigated primary processes of photoinduced ET in one of the most typical photoconductive vinyl polymers, poly(*N*-vinylcarbazole) (PVCz) and its related systems by means of picoseconds transient absorption spectroscopy and dichroism measurement in solid amorphous phase [18–21] as well as in solution phase [21–25]. From these results, it was demonstrated that rapid hole migration with time constants of 0.2 ns to a few nanosecond takes place in solution as well as in solid films. In addition, ET dynamics in rather polar solutions was well reproduced by the simple one-dimensional random walk model that rapid hole migration occurs through pendant aromatic groups with the charge recombination (CR) at the initial position of the charge separation. This scheme draws several characteristic features of the ET dynamics. First, this simple model assumes the absence of effective trap site of the cation in the polymer chain. Since the dimer cation in aromatic vinyl polymer acts as an effective trap site, it is deduced that the small stabilization energy of the dimer cation is a key condition for the polymers in which the rapid hole migration

* Corresponding author. Tel.: +81-6-6850-6241; fax: +81-6-6850-6244.
E-mail address: miyasaka@chem.es.osaka-u.ac.jp (H. Miyasaka).

1010-6030/$ – see front matter © 2003 Elsevier B.V. All rights reserved.
doi:10.1016/S1010-6030(03)00274-0

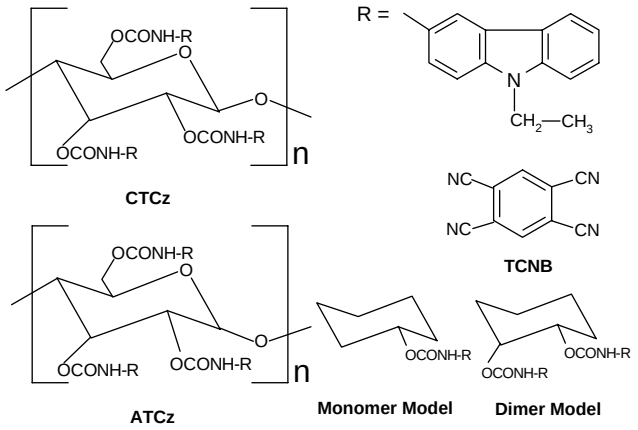

Fig. 1. Chemical structures of the compounds used.

occurs. Secondly, from the viewpoint of the reaction kinetics, it is an important condition for the rapid hole transfer (HT) process that the time constant of HT is faster than that of the micro-Brownian motion of the polymer chain leading to the conformational change for the stable dimer cation formation between side aromatic groups.

In order to directly confirm the above presumptions based on the role of dimer cation in the HT process, we have investigated the electron transfer dynamics of cellulose tris(9-ethylcarbazolyl-3-carbamate) (CTCz) and amylose tris(9-ethylcarbazolyl-3-carbamate) (ATCz) in the present work. This polymer has some characteristic features as shown in Fig. 1. Each six-membered glucoside ring of the polymer backbone contains three carbazole units attached in the 2-, 3- and 5-positions of the ring. Two of them are in a close proximity while the other one stays apart, which may cause different degrees of interaction between the neighboring Cz moieties in the polymer chain. Therefore, investigation on the ET dynamics in these characteristic polymers may provide the information on the detailed mechanism of the hole transfer process as well as the nature of the trap site for the hole. In the following, we will discuss the photoprimary processes in CTCz, ATCz as well as the corresponding monomer and dimer model systems, by integrating the present results with those accumulated for the general transient ion pairs in solutions and with the primary electron transfer processes in other aromatic vinyl polymers and their related systems.

2. Experimental

A microcomputer-controlled picosecond laser photolysis system with a custom-built repetitive mode-locked Nd^{3+}:YAG laser were used for the measurements [22]. A second harmonic pulse at 532 nm with 15 ps FWHM and ca. 0.5 mJ output power was used for exciting the samples. Monitoring white light continuum was generated by focusing the fundamental light into a 10 cm D_2O–H_2O (3:1) cell. Two sets of the multichannel photodetector (Hamamatsu, S4874) combined with a polychromator were used for the detection of the monitoring light. The repetition rate of the excitation light was kept low (<0.5 Hz). Most of the data were accumulated over four measurements. Chirping of the monitoring white light continuum was corrected. For all the systems examined in the present study, the irradiation at 532 nm corresponds to the selective excitation of the ground-state charge-transfer (CT) complexes formed between electron acceptor and Cz moieties.

The chemical structures of the compounds used are shown in Fig. 1. Cellulose tris(9-ethylcarbazolyl-3-carbamate) (CTCz) and amylose tris(9-ethylcarbazolyl-3-carbamate) (ATCz) were synthesized from the corresponding polysaccharide using 3-isocyanato-9-ethylcarbazole and purified according to the method as reported previously [26]. The structure of the CTCz and ATCz consists of a sequence of glucose units linked by 1,4-glucoside bonds. From the viewpoint of stereochemistry, the structure of CTCz is different from that of ATCz; all the glucoside bonds are the β-type in CTCz, whereas in ATCz the bonds are the α-type. 1,2,4,5-Tetracyanobenzene (TCNB; Wako GR grade) was recrystallized from ethanol and sublimed before use. 1,2-Dichloroethane (1,2-DCE; Dotite, Spectrosol) and pyridine (Wako; extra pure) were used as received. All the measurements were performed under O_2 free conditions at $21 \pm 2\,^{\circ}C$.

3. Results and discussion

3.1. Photoinduced electron transfer dynamics of the monomer model system

Prior to the discussion on the polymer systems, we present photoinduced electron transfer dynamics of the monomer model system as a reference. Fig. 2(a) exhibits the time-resolved transient absorption spectra of cyclohexyl(9-ethylcarbazolyl-3-carbamate)–TCNB in 1,2-DCE solution under the selective excitation of the ground state CT complex between Cz moiety and TCNB with a picosecond 532 nm laser pulse. A sharp absorption at 468 nm in each of the spectra is safely assigned to the anion radical of TCNB ($TCNB^-$) on the basis of the coincidence of the absorption maximum and its spectral band shape to those reported previously [27–30]. On the other hand, the broad absorption bands at 715 and 785 nm are ascribable to the cation radical of carbazolyl (Cz^+) moiety in cyclohexyl(9-ethylcarbazolyl-3-carbamate) from the comparison with the reference data [22,23,31]. The time evolution of the spectra in Fig. 2(a) indicates that the excitation of the CT absorption band results in the ion pair formation (charge separation) in the excited state.

With an increase in the delay time after the excitation, the absorbance due to the charge-separated (CS) state gradually decreases as shown in Fig. 2(a). Since the relative ratio between the absorption intensity of the cation and that of the

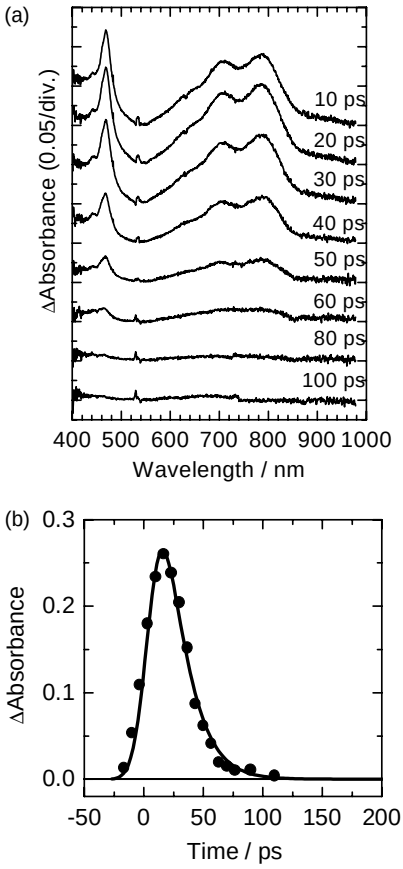

Fig. 2. (a) Time-resolved transient absorption spectra of cyclohexyl(9-ethylcarbazolyl-3-carbamate) (0.018 M)–TCNB (0.021 M) in 1,2-DCE solution, excited with a picosecond 532 nm laser pulse. (b) Time profile of the transient absorbance at 468 nm. The solid line is a convolution curve calculated by considering the pump and probe pulse widths with the time constant of ca. 16 ps.

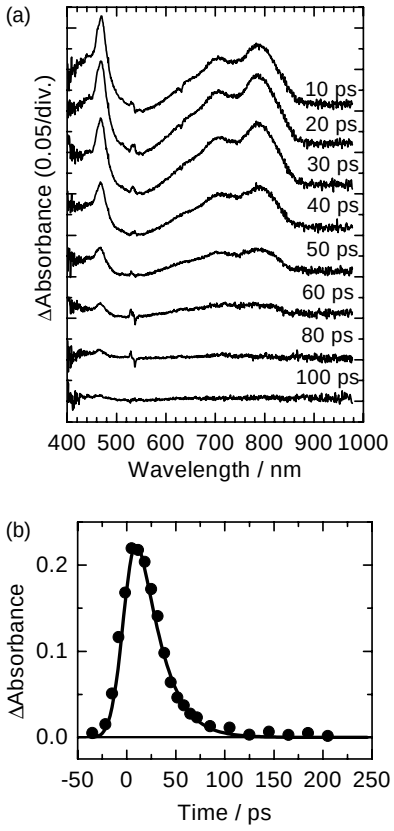

Fig. 3. (a) Time-resolved transient absorption spectra of cyclohexyl bis(9-ethylcarbazolyl-3-carbamate) ([Cz] = 0.024 M)–TCNB (0.022 M) in 1,2-DCE solution, excited with a picosecond 532 nm laser pulse. (b) Time profile of the transient absorbance at 468 nm. The solid line is a convolution curve calculated by considering the pump and probe pulse widths with the time constant of 18 ps.

anion keeps constant value during the decay process and no absorption was observed at and after ca. 100 ps following the excitation, almost all the deactivation of the ion pair was ascribed to the charge recombination (CR). Fig. 2(b) shows the time dependence of the absorbance due to the CS state monitored at 468 nm. The solid line in Fig. 2(b) is a curve calculated by taking into accounts the excitation and monitoring pulse widths and the decay time constant. The time profile was well described by the convolution curve with the decay time constant of 16 ps. The lifetime of the CS state in EtCz–TCNB system in 1,2-DCE solution was 130 ps [22]. Such a decrease of the lifetime of the CS state in the present system may be due to the introduction of the electron donating substituent into the Cz group. This substituent decreases the ionization potential of the Cz group and leads to the decrease of the energy level of the IP state. As a consequence, the energy gap between the IP state and the ground state is decreased. This results in the increase of the charge recombination rate constant with the decrease of the energy gap, which is consistent with the well-known inverted region of the bell-shaped behavior of the electron transfer reaction [1,6].

3.2. Photoinduced electron transfer dynamics of the dimer model system

Fig. 3(a) shows the time-resolved transient absorption spectra of the dimer model system, cyclohexyl bis(9-ethylcarbazolyl-3-carbamate) (CBEC)–TCNB system in 1,2-DCE solution, excited with a picosecond 532 nm laser pulse. The sharp peak at 468 nm can be ascribed to $TCNB^-$ and bands at 720 and 785 nm to Cz^+, as already mentioned in Section 3.1. Absorption spectra of the charge-separated (CS) state in the dimer model CBEC–TCNB system were quite similar to those observed in the monomer model system. The absorption intensity of anion and cation radical decreases with an increase in the delay time and almost no absorption remains at and after 100 ps following the excitation, indicating that all the CS state undergoes charge recombination to the ground state. The time profile of the CS state monitored at 468 nm is shown in Fig. 3(b). The solid line is the convolution curve with a time constant of 18 ps, which well reproduced the experimental data. This time constant is almost the same with that of the monomer model system and the rapid charge recombination process is

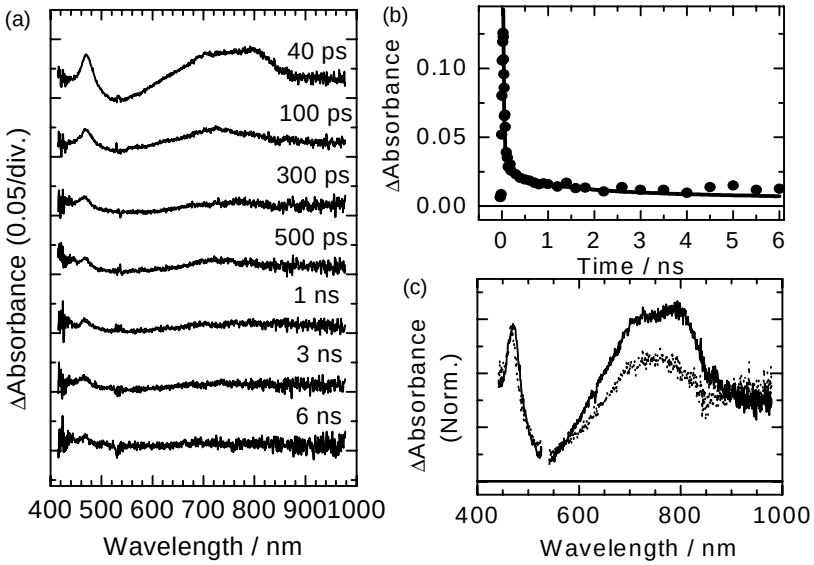

Fig. 4. (a) Time-resolved transient absorption spectra of CTCz ([Cz] = 0.018 M)–TCNB (0.020 M) in 1,2-DCE solution, excited with a picosecond 532 nm laser pulse. (b) Time profile of the transient absorbance at 468 nm. A solid line is the calculated curve based on Scheme 1 with $k_{HT} = 5.2 \times 10^8\ s^{-1}$ and $k_{CR} = 6.2 \times 10^{10}\ s^{-1}$(see text). (c) Temporal evolution of the transient absorption spectra obtained by comparing the accumulated spectrum (from 0.2 to 6 ns; dotted line) with that of 25 ps delay spectrum (solid line).

responsible for the deactivation pathway. The above results similar to those in the monomer model system indicate that the interaction between the Cz^+ and the other neighboring neutral Cz moiety was negligible in the CS state in the dimer model system.

3.3. Photoinduced electron transfer dynamics of cellulose tris(9-ethylcarbazolyl-3-carbamate) (CTCz) system in 1,2-dichloroethane solution

Fig. 4(a) exhibits the time-resolved transient absorption spectra of cellulose tris(9-ethylcarbazolyl-3-carbamate) (CTCz)–TCNB in 1,2-dichloroethane (1,2-DCE) solution, excited with a picosecond 532 nm laser pulse. As in the monomer and dimer model systems, the ground state CT complex formed between TCNB and the Cz moiety was selectively excited also in the polymer system. Each of the spectra shows a sharp absorption peak at 468 nm ($TCNB^-$) and a broad band with maxima at 710 and 790 nm (Cz^+). Although the charge-separated (CS) state in the monomer and dimer model systems completely decreased in several tens of picoseconds time region, the absorption signal of the CS state in the CTCz system was observed even in the several nanoseconds after the excitation. In addition, the absorption maximum of Cz^+ at and after several hundreds of picoseconds following the excitation was observed around 720 nm. Such a temporal evolution of the band shape of Cz^+ was not observed in the monomer or dimer model systems. This spectral evolution in the polymer system will be discussed in a later section and we will discuss the long-living CS state in the following section.

In general, the increase in the interionic distance in the ion pair to reduce the electronic tunneling matrix element for the charge recombination is indispensable for the generation of the long-lived CS state [2,32,33]. Actually, it was observed that the hole-migration process through pendant aromatic groups leading to the increase in the interionic distance resulted in the long-lived CS state formation in several nanoseconds time region for aromatic vinyl polymers—electron acceptor systems in rather polar solutions [21–25]. In addition, for these systems, the time profile of the CS state was found to be reproduced by the model that the cation radical continuously migrates along pendant aromatic moieties in polymer chain with the charge recombination at the initial position of the charge separation as shown in Scheme 1 [21–25]. Hence, we employed this scheme for the analysis of the dynamic behaviors of CTCz–TCNB in 1,2-DCE solution. As was assumed in previous analyses, all of the hole transfer rate constants (k_{HTi}) were set to be the same (k_{HT}) in the calculation. In addition, the charge recombination was assumed to take place only between $TCNB^-$ and D_0^+ (at the initial position of the charge separation) and the rate constant of the charge recombination (k_{CR}) was set to be equal to that of the monomer model system in 1,2-DCE solution. Hence, the parameter in the calculation was only the k_{HT} value.

Although this simple scheme reproduced the dynamic behavior of the CS state between aromatic vinyl polymers, such as poly(*N*-vinylcarbazole)–, poly(*N*-vinylbenzocarbazole)–, and poly(vinylnaphthalene)– electron acceptor systems in rather polar solutions, some deviation between the experimental and calculated results was observed for the present CS state between CTCz–TCNB in 1,2-DCE solution. One example of the analyzed results is shown in Fig. 4(b), where the k_{HT} value of $5.2 \times 10^8\ s^{-1}$ was used. As shown in Fig. 4(b), the experimental data was well reproduced in the subnanosecond time region, whereas one can find the

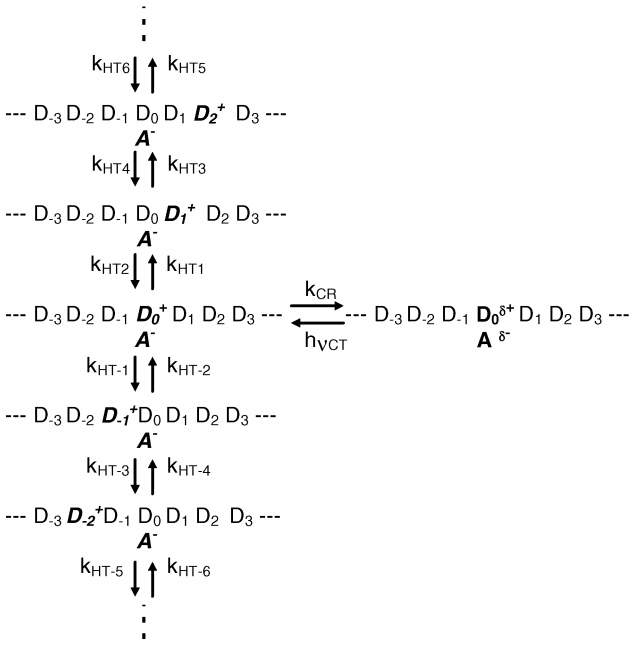

Scheme 1.

deviation of the calculated curve from the experimental result in several nanoseconds time region in such a manner that the CS state populations in the experimental results were larger than the calculated curve. The dynamic behaviors in subnanosecond time region comprise the electron transfer processes taking place in positions rather close to the initial site of the charge separation, such as the hole transfer reaction from the initial ion pair in competition with the charge recombination and the returning process of the escaped hole to the initial position of the charge separation. On the other hand, hole-returning process from the distant sites occurs in the several nanoseconds time region. The apparent deviation in the several nanoseconds time region shown in Fig. 4(b) indicates that the hole-returning processes from rather distant sites were suppressed and led to the decrease of the charge recombination process at the initial position of the charge separation.

In relation to this deviation, it is worth mentioning the temporal evolution of the absorption of the cation as explained for Fig. 4(a). In order to elucidate the relation between the deviation and the spectral evolution, we show the spectrum at 25 ps (solid line) and that averaged over nanosecond time region (dotted line) in Fig. 4(c). This figure indicates that initially observed two broad bands with maxima at 710 and 790 nm evolved in time into one single broad band with maximum at ca. 720 nm in longer time region where the deviation was observed. According to the detailed investigations on the band shape of the cation radical in aromatic vinyl polymers and its related compounds [13,34], it was demonstrated that this 720 nm band is due to the partially overlapped dimer cation of Cz moieties. The deviation in the time profile as shown in Fig. 4(b) can thus be interpreted as due to such dimer formation process. That is, the formation of the dimer cation acting as the trap site in the hole migration process resulted in the suppression of the returning of the hole to the initial position of the charge separation leading to the slower charge recombination (CR). As a result of less chance of the CR process, the population of the CS state in the experimental results was larger than that obtained by the calculation where no trap site was taken into account.

On the dimer cation formation process, it should be mentioned here that no temporal evolution of the Cz^+ was observed in the dimer model compound indicating the lack of dimer cation formation as shown in Fig. 3. On the other hand, the production of the dimer cation was observed in the polymer system. This difference may be accounted for in the following ways. First, the lifetime of the CS state in the dimer model system was very short (18 ps), whereas the CS state lifetime in the polymer system was much larger owing to the hole migration process. In addition, the HT rate constant ($5.2 \times 10^8\ s^{-1}$) was rather small. At the initial position of the charge separation, the small HT rate constant (the long staying time) leads to the charge recombination process. However, the hole once escaped from the initial CS state via the hole transfer may have chance to produce the dimer cation at the dimer site because of its long staying time.

The formation of the dimer cation generally requires the geometrical rearrangement leading to the favorable conformation. In the polymer system, the side chain dynamics may take an important role on such conformation. Although it is rather difficult to obtain the time constant of this chain dynamics at the present stage of investigation, the local conformational rearrangement in the polymer takes place in the time region of a few hundreds of picoseconds to a few nanoseconds. Since the staying time of the cation at one site was estimated to be ca. 2 ns, or ($5.2 \times 10^8\ s^{-1}$), it seems plausible for the dimer site to take a conformation favorable for the dimer cation. Actually, the fact that the spectral evolution took place in several hundreds pecoseconds to about a few nanoseconds time region supports the above discussion.

3.4. Photoinduced electron transfer dynamics of cellulose tris(9-ethylcarbazolyl-3-carbamate) (CTCz) system in pyridine solution

In this section, we discuss the electron transfer dynamics of CTCz in more polar pyridine solution. Fig. 5(a) exhibits the time-resolved transient absorption spectra of CTCz–TCNB system in pyridine solution excited with a pecosecond 532 nm laser pulse. Excitation of CT band results in the formation of the charge-separated (CS) state in the excited state. As in previous sections, we can safely attribute the sharp absorption at ca. 470 nm for $TCNB^-$ and the broad band with maxima at 710 and 785 nm for Cz^+, respectively. Similar spectral evolution as in the CTCz system was observed

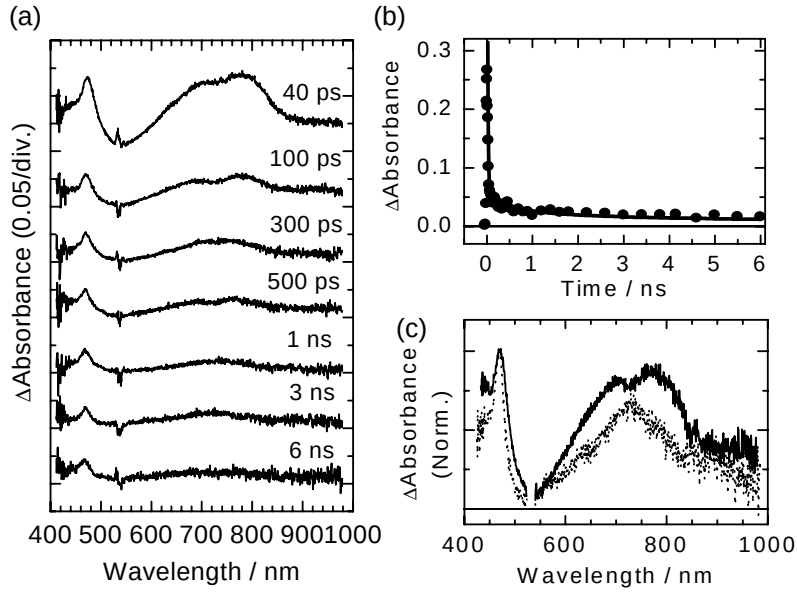

Fig. 5. (a) Time-resolved transient absorption spectra of cellulose tris(9-ethylcarbazolyl-3-carbamate) ([Cz] = 0.024 M)–TCNB (0.132 M) in pyridine solution, excited with a picosecond 532 nm laser pulse. (b) Time profile of the transient absorbance at 470 nm. A solid line is the calculated curve based on Scheme 1 with $k_{HT} = 8.0 \times 10^8\,s^{-1}$ and $k_{CR} = 6.5 \times 10^{10}\,s^{-1}$ (see text). (c) Temporal evolution of the transient absorption spectra obtained by comparing the accumulated spectrum (from 0.2 to 6 ns; dotted line) with that of 25 ps delay spectrum (solid line).

for the Cz^+ absorption band at and after 200 ps following the excitation, where the absorption band locates at around 720 nm. Compared to the results in 1,2-DCE solution, the residual absorption in the several nanoseconds time region is larger in pyridine solution. This long-lived CS state can be attributed as due to the hole escape process and the solvent polarity enhances the production of such long living ionic species.

Fig. 5(b) exhibits the time profile of the CS state monitored at 470 nm indicating the absorption signal appearing immediately after the excitation is followed by a decrease in the several tens of picoseconds time region and a much slower one in the nanosecond region. The solid curve in this figure was calculated on the basis of Scheme 1. In the calculation, the charge recombination rate constant was set to be the same as that for the monomer model system, $6.5 \times 10^{10}\,s^{-1}$. The calculated curve with $k_{HT} = 8.0 \times 10^8\,s^{-1}$ reproduces the experimental results in the subnanosecond time region together with deviation in the several nanosecond time region. The experimental results are found to be larger than the calculated curve as observed for the CTCz system in 1,2-DCE solution. This deviation can be interpreted as due to the slow returning process of the hole as a result of the dimer cation formation. Actually, as shown in Fig. 5(c), the initially formed two bands for Cz cation spectrum at 710 and 790 nm (solid line) evolved into one band at 720 nm (dotted line). Summarizing earlier in Section 3, it is concluded that similar dynamic behaviors as observed in 1,2-DCE solution took place also in pyridine solution and the HT rate constant in pyridine was slightly larger than that in 1,2-DCE.

3.5. Photoinduced electron transfer dynamics of amylose tris(9-ethylcarbazolyl-3-carbamate) (ATCz) system in pyridine solution

Fig. 6(a) shows the time-resolved transient absorption spectra of ATCz–TCNB system in pyridine solution excited with a picosecond 532 nm laser pulse. It should be mentioned here that the low solubility of ATCz did not allow us to investigate the dynamic behaviors in 1,2-DCE solution. The absorption peak at ca. 470 nm and broad band with maxima at 710 and 790 nm can be, respectively, assigned to the $TCNB^-$ and Cz^+ as explained in the previous sections. Absorption band shape and position of the CS state of ATCz system are similar to that in CTCz system.

Fig. 6(b) exhibits the decay profile of the CS state monitored at 470 nm. A fast decay within 100 ps is followed by a slow decay in nanosecond time region. The solid line shows the calculated curve based on Scheme 1 with $k_{HT} = 5.0 \times 10^8\,s^{-1}$, which reproduced the experimental results in the subnanosecond time region and a deviation was found in the nanosecond time region as in the CTCz system. The comparison of the accumulated spectrum (dotted line) in longer delay time with that of 25 ps spectrum (solid line) is shown in Fig. 6(c). The spectral evolution of the Cz^+ was also observed in the ATCz–TCNB system. From the time profile as well as spectral evolution, it is concluded that the dimer cation formation takes place also in the ATCz system in pyridine solution and the apparent deviation in the time profile is due to such dimer cation state formation acting as a trap site of the cation.

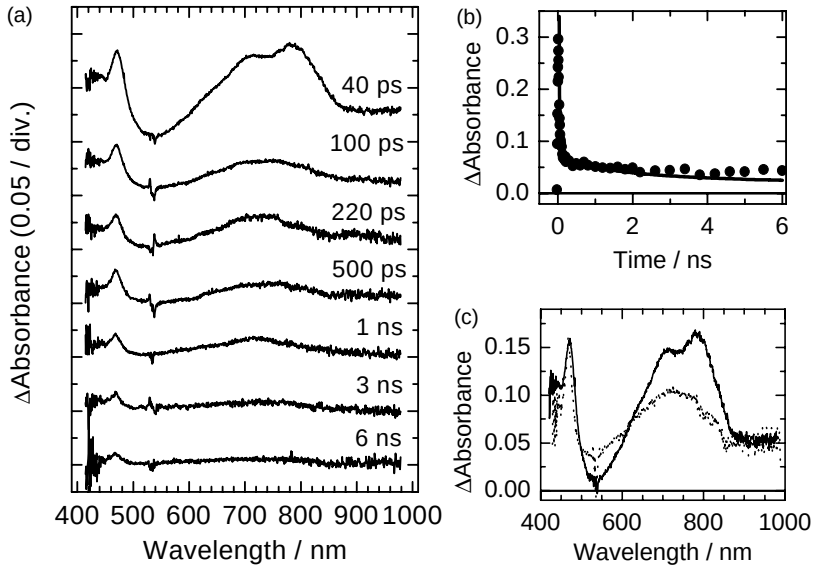

Fig. 6. (a) Time-resolved transient absorption spectra of ATCz ([Cz] = 0.024 M)–TCNB (0.126 M) in pyridine solution, excited with a picosecond 532 nm laser pulse. (b) Time profile of the transient absorbance at 470 nm. A solid line is the calculated curve based on Scheme 1 with $k_{HT} = 5.0 \times 10^8\ s^{-1}$ and $k_{CR} = 6.5 \times 10^{10}\ s^{-1}$(see text). (c) Temporal evolution of the transient absorption spectra obtained by comparing the accumulated spectrum (from 0.2 to 6 ns; dotted line) with that of 25 ps delay spectrum (solid line).

It is worth mentioning here that the extent of deviation in calculated curve from the experimental results of ATCz system in nanosecond time region is larger than that of CTCz system. This might be due to smaller HT rate constant in ATCz system. The large HT rate constant may assist the hole escape reaction but at the same time the returning process takes place quickly. In addition, the large HT rate constant decreases the chance of the side chain rearrangement to take conformation favorable for the dimer cation.

3.6. Comparison with the dynamic behaviors in PVCz systems

The HT rate constants of PVCz–TCNB systems were $2.0 \times 10^9\ s^{-1}$ in 1,2-DCE solution and $4.3 \times 10^9\ s^{-1}$ in pyridine solution [15]. On the other hand, the HT rate constants in CTCz and ATCz are almost one order smaller than those in PVCz systems. The small HT rate constants in the present system may be accounted for by the large distance between the Cz moieties. Actually, smaller HT rate constant was found also for the alternative copolymer systems with *N*-vinylcarbazole where the distance between Cz moieties was estimated to be larger than that in PVCz [35]. In addition, our previous results on the relation between the size of the aromatic groups and the HT rate constant in vinyl polymers indicated that the large HT rate constants were obtained for the polymer with large aromatic groups [21–24]. This result indicates that the short distance and the overlap of the aromatic groups are favorable condition for the rapid HT process, which is in agreement with the present result.

In the present system, the simple kinetic model of Scheme 1 did not reproduce the time profile of the electron transfer dynamics in longer delay time following the excitation. This result was interpreted as due to the trapping process of the hole at the dimer site, where the dimer cation was produced and it prevented the cationic state for returning to the initial position of the charge separation resulting in the charge recombination. The temporal evolution of the Cz^+ absorption spectra assisted the above interpretation. On the other hand, much better agreement between the experimental results and the calculated curves was observed for the electron transfer dynamics in the PVCz system in pyridine as well as in 1,2-DCE solutions. It is well known that various dimer cations are effectively produced in the vinyl homo polymers containing pendant aromatic groups, and it has been proposed that the hole is trapped at the dimer cation sites in these polymers [13]. On this point, it is worthy noting the relation between the HT rate constant and the dimer cation formation process. Since the stable dimer cation formation requires conformational rearrangement of the local structures in the polymer chain, the large HT rate constant or short staying time at one site does not allow such conformational rearrangement resulting in the stable dimer cation formation in PVCz. On the other hand, in the present CTCz and ATCz systems, the small HT rate constants resulted in the dimer cation formation at the dimer site. In addition, it is worth mentioning here that the cationic state is trapped at the site, which is relatively stable compared to other sites. There are at least two distinct sites in the present polymers as was shown in Fig. 1; two of Cz moieties are in a close proximity, whereas the other one stays apart. On the other hand, such distinction was not so clear in PVCz. In addition, delocalization of the cationic state over several Cz moieties was suggested

in PVCz systems [25]. As a result of these differences, the rapid HT processes were observed in PVCz.

4. Concluding remarks

We have investigated the photoinduced ET dynamics of CTCz, ATCz and their corresponding monomer as well as dimer model compounds in 1,2-DCE and pyridine solutions. In these polymer systems, initially formed monomer cationic state gradually evolved into dimer cationic species, as confirmed form the transient absorption spectral analysis. Formation of the dimer cation, which acts as a trap site, actually prevented the hole transfer process and led to the deviation from the simple one-dimensional random work model of the hole migration.

Acknowledgements

The present work was partly supported by the Grants-in-Aid (Nos. 14050061 and 14340183) from the Ministry of Education, Culture, Sports, Science and Technology of Japan.

References

[1] N. Mataga, Pure Appl. Chem. 65 (1993) 1606.
[2] R.A. Marcus, N. Sutin, Biochem. Biophys. Acta 811 (1985) 265.
[3] I. Rips, J. Klafter, J. Jortner, in: J.R. Norris, D. Meisel (Eds.), Photochemical Energy Conversion, Elsevier, New York, 1988, p. 1.
[4] P.F. Barbara, W. Jarzeba, Adv. Photochem. 15 (1990) 1.
[5] K. Maruyama, A. Osuka, N. Mataga, Pure Appl. Chem. 66 (1994) 867.
[6] N. Mataga, H. Miyasaka, Prog. React. Kinet. 19 (1994) 317.
[7] J. Mort, G. Pfister, in: J. Mort, G. Pfister (Eds.), Electronic Properties of Polymers, Wiley, New York, 1982, p. 215 (and references cited therein).
[8] M. Van der Auweraer, F.C. De Schryver, P.M. Borsenberger, H. Bässler, Adv. Mater. 3 (1994) 199 (and references cited therein).
[9] R.C. Penwell, B.N. Ganguly, T.W. Smith, J. Polym. Sci., Macromol. Rev. 13 (1978) 63.
[10] J.M. Peason, M. Stolka, Poly(*N*-vinylcarbazole), Gordon and Breach Science Publishers, New York, 1981.
[11] F.C. De Schryver, J. Vandendriessche, S. Toppest, K. Demeyer, N. Boens, Macromolecules 15 (1982) 406.
[12] H. Masuhara, N. Tamai, N. Mataga, F.C. De Schryver, J. Vandendriessche, J. Am. Chem. Soc. 105 (1983) 7256.
[13] H. Masuhara, A. Itaya, in: E. Tsuchida (Ed.), Macromolecular Complexes: Dynamic Interactions and Electronic Processes, VCH, New York, 1991, pp. 61–92.
[14] G. Pfister, D.J. Williams, J. Chem. Phys. 61 (1974) 2416.
[15] A. Itaya, K. Okamoto, S. Kusabayashi, Polymer. J. 17 (1985) 557.
[16] M. Yokoyama, N. Endo, H. Mikawa, Bull. Chem. Soc. Jpn. 49 (1976) 1538.
[17] G.E. Johnson, J. Chem. Phys. 62 (1975) 4697.
[18] H. Miyasaka, T. Moriyama, S. Kotani, R. Muneyasu, A. Itaya, Chem. Phys. Lett. 225 (1994) 315.
[19] H. Miyasaka, T. Moriyama, T. Ide, A. Itaya, Chem. Phys. Lett. 292 (1998) 339.
[20] A. Itaya, T. Kitagawa, T. Moriyama, T. Matsushita, H. Miyasaka, J. Phys. Chem. B 101 (1997) 524.
[21] H. Miyasaka, T. Moriyama, S. R. Khan, A. Itaya, in: F.C. De Schryver, S. De Feyter, G. Schweitzer (Eds.), Femtochemistry, Wiley–VCH, New York, 2001, pp. 335–344.
[22] H. Miyasaka, T. Moriyama, A. Itaya, J. Phys. Chem. 100 (1996) 12609.
[23] H. Miyasaka, T. Moriyama, A. Itaya, J. Phys. Chem. B 101 (1997) 10726.
[24] T. Moriyama, K. Monobe, H. Miyasaka, A. Itaya, Chem. Phys. Lett. 275 (1997) 291.
[25] H. Miyasaka, S.R. Khan, A. Itaya, J. Phys. Chem. A 106 (2002) 2192.
[26] T. Kubota, C. Yamamoto, Y. Okamoto, J. Am. Chem. Soc. 122 (2000) 4056.
[27] H. Masuhara, N. Mataga, Chem. Phys. Lett. 6 (1970) 608.
[28] H. Miyasaka, S. Ojima, N. Mataga, J. Phys. Chem. 93 (1989) 3380.
[29] S. Ojima, H. Miyasaka, N. Mataga, J. Phys. Chem. 94 (1990) 4147.
[30] S. Ojima, H. Miyasaka, N. Mataga, J. Phys. Chem. 94 (1990) 5834.
[31] T. Shida, Y. Nosaka, T. Kato, J. Phys. Chem. 82 (1978) 695.
[32] S. Kotani, H. Miyasaka, A. Itaya, J. Phys. Chem. 99 (1995) 13063.
[33] S. Kotani, H. Miyasaka, A. Itaya, J. Phys. Chem. 100 (1996) 19898.
[34] H. Masuhara, K. Yamamoto, N. Tamai, K. Inoue, N. Mataga, J. Phys. Chem. 88 (1984) 3971.
[35] S.R. Khan, T. Moriyama, K. Yamada, A. Itaya, T. Okada, H. Miyasaka, in preparation.